

Stresses in Isotropic and Anisotropic Beams Having Holes

By

Ken-ichi HIRASHIMA*

(Received September 27, 1971)

Synopsis

A theoretical analysis of stresses is presented for isotropic and anisotropic beams having holes. The beams are loaded by pure bending or cantilever bending. In the case of an isotropic body, the coefficients of mapping function are able to take a sufficient number of terms for an opening of arbitrary shapes in beams. Numerical examples are shown for the cases of isotropic beams with a hole of square, rectangular or hexagonal shape, and for the case of orthotropic beams with a hole of circular or elliptical shapes. The results obtained are valid, if the hole is small in size compared with the height of the beam.

1. Introduction

The effect of a hole on the stress distribution in isotropic elastic beams has been analysed by many investigators, e.g. Tuji¹⁾, Savin²⁾, Joseph and Brock³⁾, Heller⁴⁾, Heller et al⁵⁾, Yamasaki and Gotoh⁶⁾, and Deresiewicz⁷⁾. In these studies, the investigators treated the case of isotropic elastic beams which have a hole of circular, elliptical, triangular, square, rectangular or hexagonal shapes, subjected to pure bending or to cantilever bending. In each case the axis of the hole is perpendicular to the longitudinal axis of the beam parallel to the axis of the applied load, and the dimensions of the hole are assumed to be small compared with the width of the beam containing the hole. Thus, the problem can be treated as one of the plane stress problems of simple connected region with the single closed contour corresponding to the perforation.

On the other hand, the problem of anisotropic beams without an opening has been solved by Lekhnitskii⁸⁾, Silverman⁹⁾, and Hashin¹⁰⁾. Lekhnitskii⁸⁾, Green and Zerna¹¹⁾ have given the exact solution of plane problems for anisotropic infinite plate which have an opening of circular or elliptical shape under pure bending applied at infinity.

In the present paper, the author deals with the plane problems of stress dis-

* Department of Civil Engineering

tribution in isotropic elastic beams having a hole of arbitrary shapes and in anisotropic elastic beams having a hole of circular or elliptical shape. Owing to the proposed method by the author for the case of isotropic beams, it is not restricted to a sufficient number of terms for the coefficients of mapping function which represent an opening of arbitrary shapes. And then stress distributions are illustrated for anisotropic beams having a hole of circular or elliptical shape subjected to the complicated loads as well as pure bending.

The present work is still concerned with a certain class of generalized plane stress problem for isotropic or anisotropic elastic long beams in which the size of the hole is small compared with the width of beams. Noting with this fact, evaluations of error are examined numerically when the dimensions of the hole are enough to increase toward the width of the beam. Finally, the paper treats with the problems of beams with two or three holes in a line under pure bending applied at infinity, by the use of the method indicated in reference (12).

2. Basic Equations for Plane Anisotropic Elastic Problems

In a homogeneous and anisotropic body in plane elasticity the stress-strain relation can be written as

$$\left. \begin{aligned} \varepsilon_x &= a_{11} \sigma_x + a_{12} \sigma_y + a_{16} \tau_{xy}, \\ \varepsilon_y &= a_{12} \sigma_x + a_{22} \sigma_y + a_{26} \tau_{xy}, \\ \gamma_{xy} &= a_{16} \sigma_x + a_{26} \sigma_y + a_{66} \tau_{xy}, \end{aligned} \right\} \quad (2.1)$$

where the a_{ij} 's are the elastic compliances.

In the case where the material is isotropic, the a_{ij} 's may be expressed in terms of the Young's modulus E_0 and Poisson's ratio ν_0 as follows

$$\left. \begin{aligned} a_{11} &= a_{22} = 1/E_0, & a_{12} &= -\nu_0/E_0, \\ a_{16} &= a_{26} = 0, & a_{66} &= 2(1+\nu_0)/E_0. \end{aligned} \right\} \quad (2.2)$$

It may be shown that the stresses in an anisotropic body can be given in terms of two functions of complex variables:

$$z_1 = x + \mu_1 y, \quad z_2 = x + \mu_2 y, \quad (2.3)$$

μ_1, μ_2 and their complex conjugates $\bar{\mu}_1, \bar{\mu}_2$ are the roots of characteristic equation for the anisotropic body under consideration as follow:

$$a_{11} \mu^4 - 2a_{16} \mu^3 + (2a_{12} + a_{66}) \mu^2 - 2a_{26} \mu + a_{22} = 0. \quad (2.4)$$

The stress components in rectangular Cartesian coordinates (x, y) are expressed in

terms of two complex stress functions $\phi_1'(z_1)$ and $\phi_2'(z_2)$ ⁸⁾.

$$\left. \begin{aligned} \sigma_x &= 2R_e [\mu_1^2 \phi_1'(z_1) + \mu_2^2 \phi_2'(z_2)], \\ \sigma_y &= 2R_e [\mu_1 \phi_1'(z_1) + \phi_2'(z_2)], \\ \tau_{xy} &= -2R_e [\mu_1 \phi_1'(z_1) + \mu_2 \phi_2'(z_2)]. \end{aligned} \right\} \quad (2.5)$$

When the material is isotropic, we obtain the well-known formulae of Kolosov-Muskhelishvili¹³⁾:

$$\left. \begin{aligned} \sigma_y - \sigma_x + 2i \tau_{xy} &= 2 [z_0 \varphi''(z_0) + \psi'(z_0)], \\ \sigma_x + \sigma_y &= 4R_e [\varphi'(z_0)]. \end{aligned} \right\} \quad (2.6)$$

When the Cartesian coordinates (x, y) are taken as Fig. 1~3, stress distributions in an anisotropic beam without a hole subjected to pure bending or to cantilever bending are as follows^{*8,10)}.

(1) Pure Bending

When the beam having no hole subjects to end couples M , stresses in this case are as follows:

$$\sigma_x^o = -\frac{M}{I} (y + \varepsilon_0), \quad \sigma_y^o = \tau_{xy}^o = 0, \quad (2.7)$$

where I is the moment inertia around a center of the beam, and ε_0 is excentricity from the center line of the beam to the coordinate axis x as shown in Fig. 1.

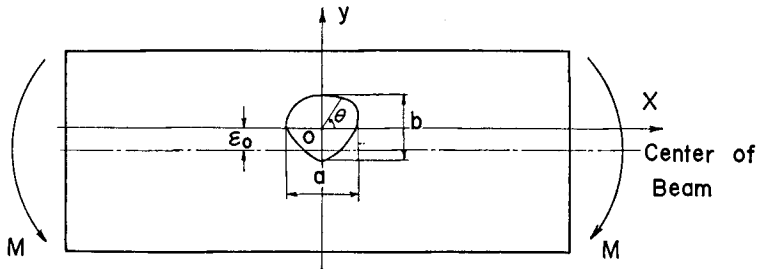


Fig. 1. Beam with a hole subjected to pure bending.

* Hashin¹⁰⁾ has obtained the theoretical solution for anisotropic elastic beams in a state of plane stress using the method of double polynomial series developed by Neou¹⁴⁾. Though he points out that the solution for stresses as given by Lekhnitskii are not correct, we can not find the errors in the Lekhnitskii's original Russian book (second ed.)¹⁵⁾ and its English translation⁸⁾. It may be thought that the errors suggested by Hashin are due to the misprints of the English book¹⁶⁾ or the original Russian book (first ed.).

(2) Cantilever Beam by a Terminally Concentrated Load

A beam with a rectangular cross section is fixed at one end and is bent by a transverse force P applied to the other end (see Fig. 2). In this case stress components are expressed as follows.

$$\left. \begin{aligned} \sigma_x^o &= \frac{P}{I} \left[(a_0 - x) (y + \varepsilon_0) + \frac{a_{16}}{a_{11}} \left\{ \frac{h^3}{3} - (y + \varepsilon_0)^2 \right\} \right], \\ \sigma_y^o &= 0, \quad \tau_{xy}^o = -\frac{P}{I} \{ h^2 - (y + \varepsilon_0)^2 \}. \end{aligned} \right\} \quad (2.8)$$

Among these components, σ_y^o and τ_{xy}^o are identical to those in the case of an anisotropic beam. In an orthotropic beam where the direction of the x -axis is the principal direction of elasticity $a_{16}=0$ and also stress σ_x^o is practically the same value as for an isotropic beam. In the case of a beam for which compliance a_{16} is not equal to zero (i.e. in the case of an anisotropic or an orthotropic beam where the axial direction x is not a principal direction), stress is distributed across the cross section not linearly, but parabolically.

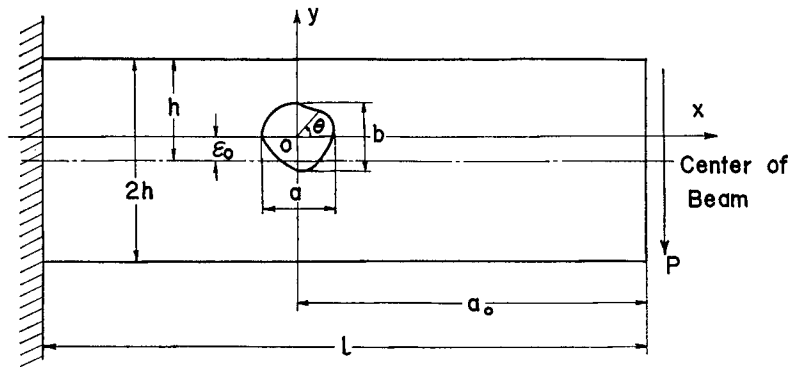


Fig. 2. Cantilever beam with a hole subjected to a terminally concentrated load.

(3) Cantilever Beam by a Uniformly Distributed Load

A beam with a rectangular cross section is fixed at one end and is bent by a normal load q (per unit length) uniformly distributed on upper side of the beam (see Fig. 3). We obtain the following formulae for the stress components;

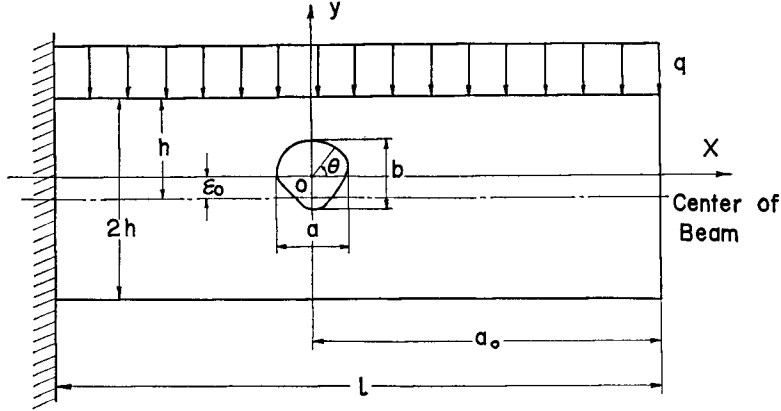


Fig. 3. Cantilever beam with a hole subjected to a uniformly distributed load.

$$\begin{aligned}
 \sigma_x^o &= \frac{q}{6I} \left[\left\{ 3y(a_0 - x)^2 + 2\lambda(a_0 - x)(h^2 - 3y^2) + 2\xi \left(-\frac{3}{5}h^2 - y^2 \right) y \right\} \right. \\
 &\quad \left. + \varepsilon_0 \left\{ 3(a_0 - x)^2 - 6\lambda(a_0 - x)(2y + \varepsilon_0) + 2\xi \left(\frac{3}{5}h^2 - 3y^2 - 3\varepsilon_0 y - \varepsilon_0^2 \right) \right\} \right], \\
 \sigma_y^o &= -\frac{q}{6I} \left\{ (2h^3 + 3h^2 y - y^3) + \varepsilon_0 (3h^2 - 3y^2 - 3\varepsilon_0 y - \varepsilon_0^2) \right\}, \\
 \tau_{xy}^o &= \frac{q}{6I} \left[(y^2 - h^2) \{ 3(a_0 - x) + 2\lambda y \} \right. \\
 &\quad \left. + \varepsilon_0 \{ 3(a_0 - x)(2y + \varepsilon_0) + 2\lambda(h^2 - 3y^2 - 3\varepsilon_0 y - \varepsilon_0^2) \} \right].
 \end{aligned} \tag{2.9 a}$$

$$\lambda = \frac{a_{16}}{a_{11}}, \quad \xi = 2 \left(\frac{2a_{12} + a_{66}}{4a_{11}} - \lambda^2 \right). \tag{2.9 b}$$

It is also obvious for this case that the distribution of σ_y^o and τ_{xy}^o in an orthotropic beam dose not differ from that in an isotropic beam.

As was shown above, when obtaining the stress distributions in an anisotropic beam without opening subjected to pure bending or to cantilever bending, stresses in the beam with an opening can be calculated as follows. Firstly, we calculate the radial normal stress and the tangential shearing stress on the virtual contour of a hole which would be perforated in the beam, from equation (2.7), (2.8) or (2.9). Then, we calculate the stresses by equation (2.5) when the external loads equal the magnitude and oposite sign of the stresses in the above are applied on the contour of a hole of the perforated beam. And then we can solve the problem under consideration by superimposing the stress components $\sigma_x, \sigma_y, \tau_{xy}$ by (2.5) to $\sigma_x^o, \sigma_y^o,$

τ_{xy}^0 by (2.7), (2.8) or (2.9). Therefore, it may be reduced to solve the first boundary value problem of simple-connected region with an opening.

3. Method of Analysis

We refer the plane body under consideration to Cartesian coordinate system (x, y) where the origin lies in an arbitrary cross section of the hole. We consider an infinite elastic plate with the hole, the contour of which is given by expression:

$$\left. \begin{aligned} x_0 &= \alpha_0 \cos \theta + \sum_{m=1}^{\nu} (\alpha_m \cos m\theta + \beta_m \sin m\theta), \\ y_0 &= \alpha_0 \sin \theta - \sum_{m=1}^{\nu} (\alpha_m \sin m\theta - \beta_m \cos m\theta). \end{aligned} \right\} \quad (3.1)$$

In which θ is a parameter varying from 0 to 2π in a counter-clockwise direction on the contour and $\alpha_m, \beta_m, (m=1, 2, \dots, \nu)$ represent the real constants to be decided by the cross section of a hole, and ν is a finite integer with plus sign. For example, it may be set $\alpha_m = \beta_m = 0, (m=1, 2, \dots, \nu)$ for a circular hole and $\beta_1 = \alpha_m = \beta_m = 0, (m=2, 3, \dots, \nu)$ for an elliptical one. Several investigators have calculated the values of the constants α_m, β_m in company with the variations of the rounded corner of an opening with several cross sections.¹⁷⁾

A complex plane $z_0 (=x+iy)$ with the hole as given by equation (3.1) is conformally transformed onto the exterior of a unit circle $|\zeta|=1$ in the ζ -plane. The mapping function is expressed as

$$z_0 = w(\zeta) = \alpha_0 \zeta + \sum_{m=1}^{\nu} (\alpha_m + i\beta_m) \zeta^{-m}. \quad (3.2)$$

Similarly, we consider the solutions of the problem by mapping the planes $z_k (=x+\mu_k y)$, as shown in equation (2.3), onto the exteriors of unit circles $|\zeta_k|=1$ in the ζ_k -planes. Then the mapping functions may be taken as:

$$\begin{aligned} z_k &= \frac{1}{2} \left[\alpha_0 \{ (1 - i\mu_k) \zeta_k + (1 + i\mu_k) \zeta_k^{-1} \} \right. \\ &\quad + \sum_{m=1}^{\nu} \{ (1 + i\mu_k) \alpha_m - i(1 - i\mu_k) \beta_m \} \zeta_k^m \\ &\quad \left. + \sum_{m=1}^{\nu} \{ (1 - i\mu_k) \alpha_m + i(1 - i\mu_k) \beta_m \} \zeta_k^{-m} \right] \quad (3.3) \end{aligned}$$

Each of these functions on the contour of the cross section of a hole takes a value equal to $\zeta = \zeta_k = \sigma (\equiv e^{i\beta})$.

If X_n and Y_n are the components of the external force related to a unit area along the axial directions of the coordinates (x, y) , two complex stress functions $\phi_k(z_k)$ appearing in equation (2.5) can be written as:

$$\left. \begin{aligned} 2R_e [\phi_1(z_1) + \phi_2(z_2)] &= \int_0^s Y_n ds + c_1, \\ 2R_e [\mu_1\phi_1(z_1) + \mu_2\phi_2(z_2)] &= - \int_0^s X_n ds + c_2. \end{aligned} \right\} \quad (3.4)$$

Where c_1, c_2 are constants which can be fixed arbitrary on the contour, since the simple-connected region is to be considered; without loss of generality with respect to this case we can set these constants equal to zero.

Whereas the external stresses X_n and Y_n along the contour of a hole can be determined by the use of the stress components of equation (2.7), (2.8) or (2.9) as follows.

$$\left. \begin{aligned} X_n &= - [\sigma_x^o \cos(n, x_o) + \tau_{xy}^o \cos(n, y_o)], \\ Y_n &= - [\tau_{xy}^o \cos(n, x_o) + \sigma_y^o \cos(n, y_o)], \end{aligned} \right\} \quad (3.5)$$

in which n is a unit vector directed to the inward normal to the contour of a hole. Using a tangential unit vector s for clockwise direction on the contour, we have

$$\cos(n, x_o) = - \frac{dy_o}{ds}, \quad \cos(n, y_o) = \frac{dx_o}{ds}. \quad (3.6)$$

Thus by substituting from equations (3.5), (3.6) and (3.1) into the right-hand sides of equation (3.4) and intergrating with respect to the arc-length from an arbitrary initial point to a variable point s , we shall assume that equation (3.4) can be expanded in a Fourier series in $e^{im\theta}$ and $e^{-im\theta}$ as

$$\left. \begin{aligned} 2R_e [\phi_1(z_1) + \phi_2(z_2)] &= + \frac{Y}{2\pi} \theta + a_o + \sum_{m=1}^{\infty} (a_m e^{im\theta} + \bar{a}_m e^{-im\theta}), \\ 2R_e [\mu_1\phi_1(z_1) + \mu_2\phi_2(z_2)] &= - \frac{X}{2\pi} \theta + b_o + \sum_{m=1}^{\infty} (b_m e^{im\theta} + \bar{b}_m e^{-im\theta}). \end{aligned} \right\} \quad (3.7)$$

Where a_m, b_m are the complex constants to be determined from applied stresses and the shape of a hole, and \bar{a}_m, \bar{b}_m are their conjugates; a_o, b_o are arbitrary constants which can be set equal to zero in our case; X, Y are the components of the resultants of the external forces acting on the contour of hole.

Assuming that the functions $\phi_k(z_k)$ are defined as the following:

$$\phi_k(z_k) = \Gamma_k l_n \zeta_k + \sum_{m=1}^{\infty} \Gamma_{km} \zeta_k^{-m}, \quad (k = 1, 2), \quad (3.8a)$$

then the complex coefficients Γ_{km} can be expressed by \bar{a}_m, \bar{b}_m as

$$\Gamma_{1m} = \frac{b_m - \mu_2 \bar{a}_m}{\mu_1 - \mu_2}, \quad \Gamma_{2m} = \frac{\mu_1 \bar{a}_m - \bar{b}_m}{\mu_1 - \mu_2}. \quad (3.8b)$$

For $m \geq 2$, however, z_k is not a suitable function, because branch points of the $z_k - \zeta_k$ transformation occur when $|\zeta| > 1$, and any function $\phi_k(z_k)$ of ζ_k such as equation (3.8) will not, in general, be single-valued throughout the region under consideration. It is necessary to make several modifications such as the methods developed by Stephens¹⁸⁾ and Lekhnitskii¹⁹⁾. The present paper will therefore treat only the problems of an anisotropic material having a circular or an elliptical hole (corresponding to $m=1$ in equation (3.3)) at which the complex functions $\phi_k(z_k)$ are singlevalued throughout the region, because z_k have no zero on or outside the unit circles $|\zeta|=1$.

On the other hand, when the material is an isotropic body, stress components σ_x, σ_y and τ_{xy} must be determined by equation (2.6). Using the formula derived in Appendix I, we can easily obtain a solution of plane problem of an isotropic body with a hole of arbitrary shapes which is given as equation (3.1).

Let us use curvilinear coordinates (ξ, η) which ξ and η define the point by means of two orthogonal intersecting curves. One of their closed curves consists of the contour of an opening under consideration. And let us specify the stresses as σ_ξ , the normal component on a curve $\xi=\text{constant}$; σ_η , the normal component on a curve $\eta=\text{constant}$; $\tau_{\xi\eta}$, the shear component on both curves. The following equations can be obtained from the fundamental relations of stresses.

$$\left. \begin{aligned} \sigma_\xi + \sigma_\eta &= \sigma_x + \sigma_y, \\ \sigma_\xi - \sigma_\eta + 2i \tau_{\xi\eta} &= \frac{\bar{\zeta}}{\zeta} \cdot \frac{d\zeta}{dz_0} \cdot \frac{d\bar{z}_0}{d\bar{\zeta}} (\sigma_x - \sigma_y + 2i \tau_{xy}). \end{aligned} \right\} \quad (3.9)$$

Where σ_x, σ_y and τ_{xy} are the stress components in rectangular Cartesian coordinates (x, y) as given by equation (2.5) or (2.6).

In the next section we will show some numerical examples of isotropic and anisotropic beams subjected to pure bending or to cantilever bending.

4. Numerical Examples

(1) Pure Bending

For the case of an anisotropic beam subjected to end couples, M (see Fig.1), the stresses in this beam having no hole are given by equation (2.7). The stresses

on the virtual contour of the hole which would be perforated in the beam may then be represented by equation (2.7) replaced y by y_0 of equation (3.1). Inserting this expression into equation (3.6), the integrations of external stresses X_n, Y_n can be expanded in a Fourier series in $\cos m\theta$ and $\sin m\theta$ by the aid of the auxiliary integrations shown in Appendix II. In this case the complex constants \bar{a}_m, \bar{b}_m in equation (3.7) are determined by

$$\left. \begin{aligned} a_m = 0, \quad b_m = \frac{M}{4I}(K_m + i L_m), \quad X = Y = 0, \\ (m = 1, 2, \dots, 2\nu) \end{aligned} \right\} \quad (4.1)$$

where,

$$\left. \begin{aligned} K_m = 2\varepsilon_0 \beta_m + F_m^1, \quad L_m = 2\varepsilon_0 d_m'' + H_m^1, \quad (\text{for } m = 1, 2, \dots, \nu), \\ K_m = F_m^1, \quad L_m = H_m^1, \quad (\text{for } m = \nu + 1, \dots, 2\nu). \end{aligned} \right\} \quad (4.2)$$

Then the stress components referred with the coordinates (x, y) can be obtained from equation (2.5) for an anisotropic case (in which it should be set ν equal to 1), or equation (2.6) for an isotropic case. And then using equation (3.9), we can get the stress components referred with the curvilinear coordinates (ξ, η) .

Let us show some typical examples for the circumferential stress at the contour of the hole of arbitrary shapes subjected to pure bending. Here, we will quote mainly the coefficients $\alpha_m, \beta_m, (m=0, 1, 2, \dots, \nu)$ of mapping functions for rectangular openings given by Heller and others¹⁷⁾, for the case of an isotropic beam. The number of the terms being adopted in these mapping functions is $\nu=7$.

Fig. 4 shows the distribution of the circumferential stress σ_η at the contour of a square hole ($k=a/b=1.0$), which is perforated in an isotropic beam under pure bending, for the variations of rounded corners ($\rho=r_0/a, r_0$; corner radius) of openings

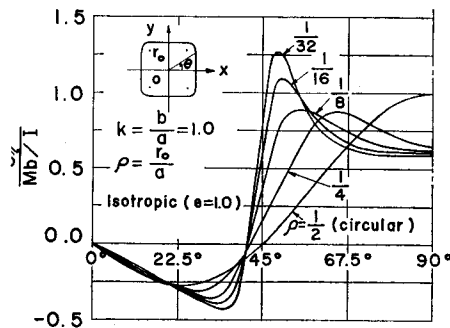


Fig. 4. Typical tangential stress distribution along edge of square hole in isotropic beam subjected to pure bending.

as the parameters. This result may be also obtained from the theoretical solution given by Heller and others. Fig. 5 shows the distribution of the circumferential stress σ_η at the contour of a circular hole which is perforated in an orthotropic beam when the ratios $e(=E_1/E_2)$ of the elastic moduli and angles φ take several typical values. In which φ is an angle in a counter-clockwise direction between the x -axis and the direction of principal elastic modulus E_1 . Left half of solid lines of this figure shows the distribution of σ_η for the case of $\varphi=0^\circ$ (i.e. $E_x=E_1, E_y=E_2$) and right half of solid lines the case of $\varphi=90^\circ$ (i.e. $E_x=E_2, E_y=E_1$). In these cases, the stress distributions are both symmetrical with respect to the line equal to $\theta=90^\circ$. The stress σ_η for the case of $\varphi=45^\circ$ is shown by dotted lines in the same figure.

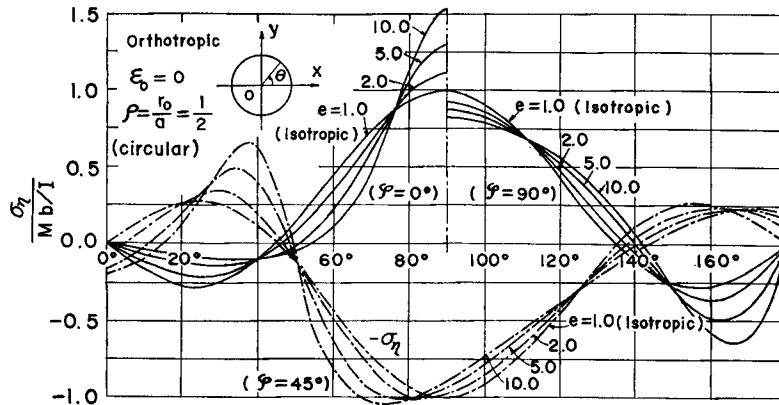


Fig. 5. Typical tangential stress distribution along edge of circular hole in orthotropic beam subjected to pure bending.

In above examples we set the elastic constants such that the Poisson's ratio ν_1 is equal to 0.15 and the shear modulus is defined as

$$\frac{1}{G_{12}} = \frac{1}{E_1} + \frac{1}{E_2} + \frac{2\nu_1}{E_1}. \quad (4.3)$$

(2) Cantilever Beam by a Terminally Concentrated Load

As was shown in Fig. 2 and preceding section, the stress distribution in a homogeneous anisotropic beam with no hole is given by equation (2.8). The stresses σ_x , σ_y and τ_{xy} on the virtual contour of the hole which would be perforated in this beam may then be represented by equation (2.8) substituted x_0 and y_0 in equation (3.1) for x and y respectively. Inserting into equation (3.5) and integrating the right-hand sides of equation (3.4), we obtain

$$\left. \begin{aligned} \bar{a}_m &= \frac{P}{8I} (Q_m^1 + i R_m^1), \quad \bar{b}_m = \frac{P}{8I} (Q_m^2 + i R_m^2), \\ &\quad (m = 1, 2, \dots, 3\nu) \\ X &= -\frac{\pi}{2} \frac{P}{I} Q_0^2, \quad Y = \frac{\pi}{2} \frac{Q}{I} Q_0^1, \end{aligned} \right\} \quad (4.4)$$

where,

$$\left. \begin{aligned} Q_0^1 &= 4\varepsilon_0 F_0^1 + M_0^1, \\ Q_m^1 &= 4(\varepsilon_0^2 - h^2) \beta_m + 4\varepsilon_0 F_m^1 + M_m^1, \quad (\text{for } m=1, 2, \dots, \nu) \\ R_m^1 &= 4(\varepsilon_0^2 - h^2) \alpha_m'' + 4\varepsilon_0 H_m^1 + N_m^1, \\ Q_m^1 &= 4\varepsilon_0 F_m^1 + M_m^1, \quad R_m^1 = 4\varepsilon_0 H_m^1 + N_m^1, \quad (\text{for } m=\nu+1, \dots, 2\nu) \\ Q_m^1 &= M_m^1, \quad R_m^1 = N_m^1, \quad (\text{for } m=2\nu+1, \dots, 3\nu) \\ Q_0^2 &= 2(\delta_1 F_0^1 + 2\varepsilon_0 F_0^2 + \varepsilon_0 F_0^3) + \lambda M_0^1 + M_0^2 + M_0^3, \\ Q_m^2 &= 4(\delta_2 \beta_m + \delta_3 \alpha_m') + 2(\delta_1 F_m^1 + 2\varepsilon_0 F_m^2 + \varepsilon_0 F_m^3) \\ &\quad + \lambda M_m^1 + M_m^2 + M_m^3, \\ R_m^2 &= 4(\delta_2 \alpha_m'' + \delta_3 \beta_m) + 2(\delta_1 H_m^1 + 2\varepsilon_0 H_m^2 + \varepsilon_0 H_m^3) \\ &\quad + \lambda N_m^1 + N_m^2 + N_m^3 \\ &\quad (\text{for } m = 1, 2, \dots, \nu) \\ Q_m^2 &= 2(\delta_1 F_m^1 + 2\varepsilon_0 F_m^2 + \varepsilon_0 F_m^3) + \lambda M_m^1 + M_m^2 + M_m^3, \\ R_m^2 &= 4(\delta_1 H_m^1 + 2\varepsilon_0 H_m^2 + \varepsilon_0 H_m^3) + \lambda N_m^1 + N_m^2 + N_m^3, \\ &\quad (\text{for } m = \nu + 1, \dots, 2\nu) \\ Q_m^2 &= \lambda M_m^1 + M_m^2 + M_m^3, \quad R_m^2 = \lambda N_m^1 + N_m^2 + N_m^3, \\ &\quad (\text{for } m = 2\nu + 1, \dots, 3\nu) \\ \delta_1 &= 2\lambda \varepsilon_0 - a_0, \quad \delta_2 = \lambda \left(\varepsilon_0^2 - \frac{h^2}{3} \right) - a_0 \varepsilon_0, \quad \delta_3 = \varepsilon_0^2 - h^2. \end{aligned} \right\} \quad (4.5a)$$

Thus the complex functions $\phi_k(z_k)$ for this case may be determined as follows.

$$\left. \begin{aligned} \phi_1(z_1) &= \Gamma_1 \ln \zeta_1 + \frac{1}{\mu_1 - \mu_2} \sum_{m=1}^{3\nu} (\bar{b}_m - \mu_2 \bar{a}_m) \zeta_1^{-m}, \\ \phi_2(z_2) &= \Gamma_2 \ln \zeta_2 - \frac{1}{\mu_1 - \mu_2} \sum_{m=1}^{3\nu} (\bar{b}_m - \mu_1 \bar{a}_m) \zeta_2^{-m}. \end{aligned} \right\} \quad (4.6)$$

In which the coefficients Γ_1 and Γ_2 in equation (4.6) are the complex constants which satisfy the following simultaneous linear equations:

$$\left. \begin{aligned} \Gamma_1 + \Gamma_2 - \bar{\Gamma}_1 - \bar{\Gamma}_2 &= -\frac{Y}{2\pi} i, \\ \mu_1 \Gamma_1 + \mu_2 \Gamma_2 - \bar{\mu}_1 \bar{\Gamma}_1 - \bar{\mu}_2 \bar{\Gamma}_2 &= \frac{X}{2\pi} i, \\ \mu_1^2 \Gamma_1 + \mu_2^2 \Gamma_2 - \bar{\mu}_1^2 \bar{\Gamma}_1 - \bar{\mu}_2^2 \bar{\Gamma}_2 &= \frac{i}{2\pi} \left(\frac{a_{16}}{a_{11}} X + \frac{a_{12}}{a_{11}} Y \right), \\ \frac{1}{\mu_1} \Gamma_1 + \frac{1}{\mu_2} \Gamma_2 - \frac{1}{\bar{\mu}_1} \bar{\Gamma}_1 - \frac{1}{\bar{\mu}_2} \bar{\Gamma}_2 &= -\frac{i}{2\pi} \left(\frac{a_{12}}{a_{22}} X + \frac{a_{26}}{a_{22}} Y \right). \end{aligned} \right\} \quad (4.7)$$

Since all the coefficients of the functions $\phi_k(z_k)$ can be completely decided as mentioned above, we can easily obtain the expressions for the stresses in the case of anisotropic beam.

In the case where the beam is an isotropic plate, the analytic functions $\varphi(z_0)$ and $\psi(z_0)$ may be determined in the manner to be shown in Appendix I.

Let us show several numerical examples. For the purposes of comparison with the results given by Savin and Deresiewicz, let it be assumed that, in each case, $l=10h=\frac{4}{3}a_0$ are retained and the dimension b of the hole normal to the longitudinal axis of the beam is one quarter of the height of the beam (i.e. $b=h/2$). Fig. 6 and Fig. 7 show the variation of σ_η in the case of several shapes of opening perforated in an isotropic beam, with various values of corner radii $\rho=r_0/a$. The variation of σ_η for the case of square hole and rectangular one ($k=a/b=2.0$) is given in Fig. 6(a), and hexagonal one in Fig. 6(b). From the fact that the mapping employed by Savin and Deresiewicz is onto the interior, and that by the author onto the exterior

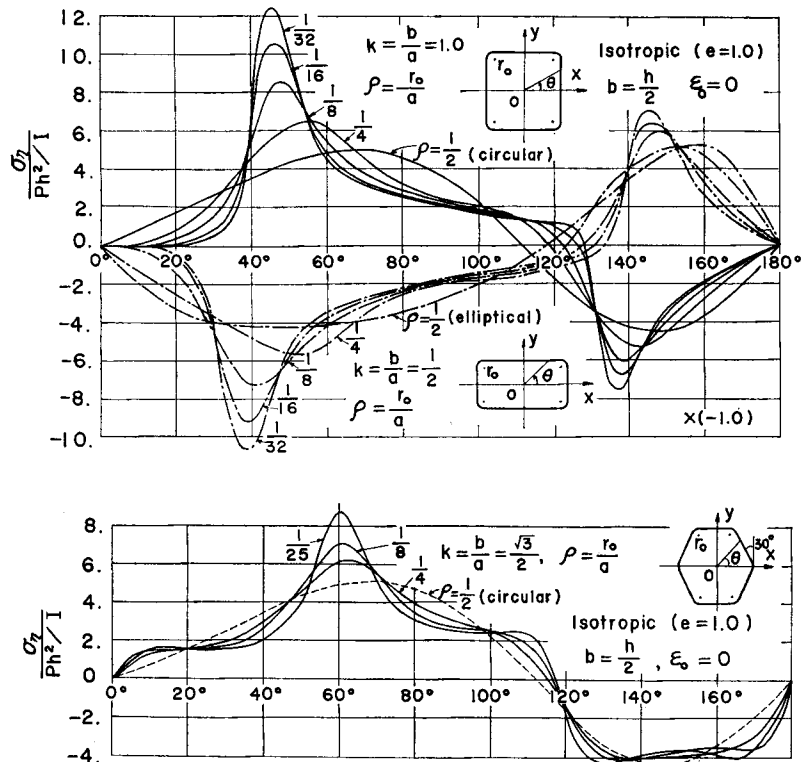


Fig. 6. Typical tangential stress distribution along edge of (a) square ($a/b=1.0$), rectangular ($a/b=2.0$) and (c) hexagonal hole in isotropic cantilever beam subjected to a terminally concentrated load.

of the unit circles, these two results in this example are slightly different except in the case of the particular shape of opening e.g. a circular opening or an elliptical one. The coefficients of mapping function to represent an opening with hexagonal shapes as in Fig. 6 (b) have been used the values given by Yamasaki and Gotoh⁶⁾. Fig. 7 shows variation of σ_η at the contour of square openings corresponding to Fig. 6 (a) with which the eccentricity ϵ_0 from the origin of opening to the center line of a beam is equal to $h/4$.

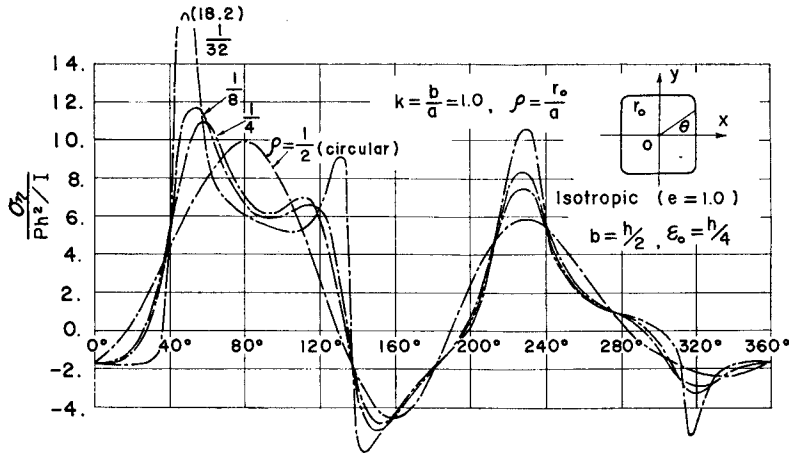
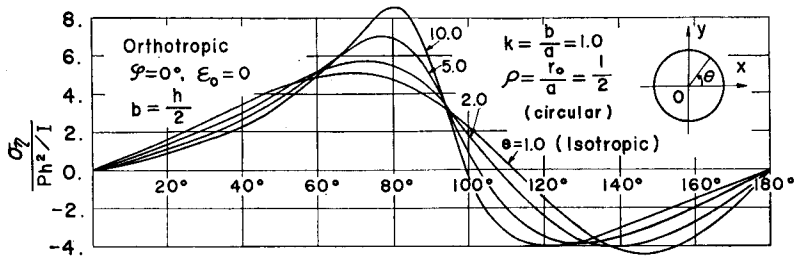


Fig. 7. Same as square holes in Fig. 6 (a), except with excentricity ($\epsilon_0=h/4$) from the center line of the beam.

Though the numerical results are only given in the above examples for an isotropic beam, those for an orthotropic beam are plotted in Fig. 8 and Fig. 9. Fig. 8 (a), and (b) show the circumferential stress σ_η at the contour of a circular opening against the variation of ratio e of the principal elastic moduli and the angle φ between the x -axis and the axis of the principal elastic modulus E_1 . Although showing the range of θ from 0 to π in Fig. 8(a), these stress distributions are in antisymmetry with respect to the x -axis. As was shown in Fig. 8 (b), when the axes of the principal



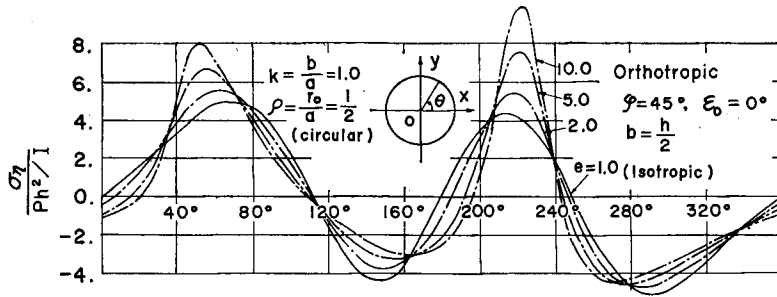


Fig. 8. Typical tangential stress distribution along edge of circular hole in orthotropic cantilever beam subjected to a terminally concentrated load.

elastic moduli do not coincide with the coordinates (x, y) , distribution of σ_τ is not in antisymmetry with respect to the x -axis. Fig. 9 are two of examples of circumferential stresses for an orthotropic beam with an eccentric opening ($\epsilon_0 = h/4$).

In the above examples we make the assumption that the orthotropic beam has the elastic constants as in the previous cases for pure bending.

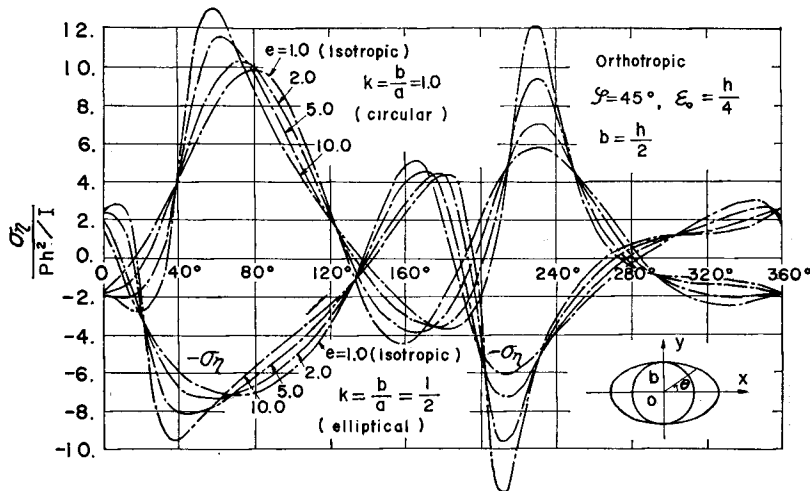


Fig. 9. Same as Fig. 8 (b), except with excentricity ($\epsilon_0 = h/4$) from the center line of the beam.

(3) Cantilever Beam by a Uniformly Distributed Load

The theoretical expressions for this case are more complicated ones in comparison with cases (1) and (2). Being able to be calculated by the same manner as the above cases, numerical expressions are omitted for this case.

Fig. 10 is the distribution of circumferential stress σ_τ at the contour of the square hole ($k = a/b = 1.0$) such that the hole is perforated at the center line of longitudinal

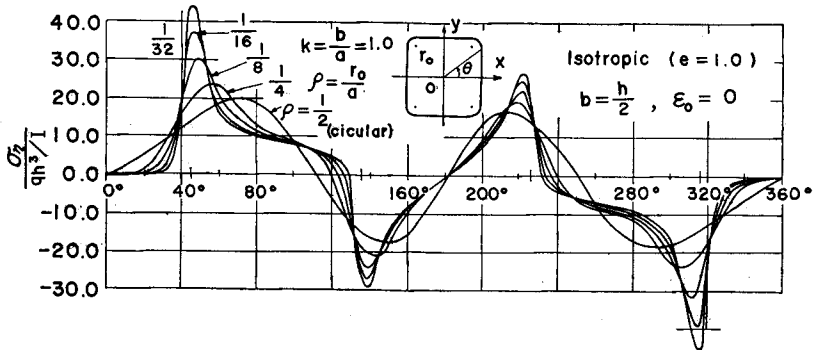


Fig. 10. Typical tangential stress distribution along edge of square hole in isotropic cantilever beam subjected to a uniformly distributed load.

axis of an isotropic beam. From this figure, it can be observed that the stress distributions are not in antisymmetry with respect to the x -axis. This reason is due to the fact that the stress component σ_y^0 caused by a uniformly distributed load on upper boundary of the beam is not in antisymmetry with respect to the center line of the beam.

As in the general case of an orthotropic beam, the distribution of circumferential stress σ_n at the contour of the circular and the elliptical hole ($a/b=2.0$) in the case of $e=5.0$, $\varphi=45^\circ$, $\epsilon_0=h/4$ are shown in Fig. 11. Dotted lines in this figure indicate the distribution of σ_n for the case where the eccentricity ϵ_0 is equal to $-h/4$ (i.e. for the case when the opening is perforated to the position downward the center line of the beam) and broken lines for the case of $\epsilon_0=h/4$. In order to easily compare with two cases of $\epsilon_0=h/4$ and $\epsilon_0=-h/4$ in the same figure, stress σ_n for the case of $\epsilon_0=-h/4$ are plotted in which the angle φ are taken in a clockwise direction and the sign of stress σ_n is taken in opposite to the true value.

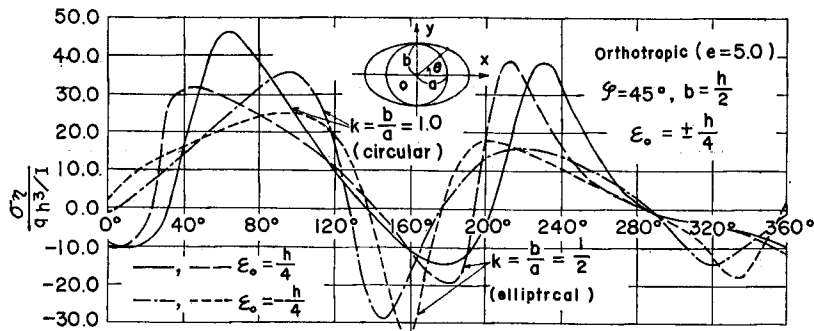


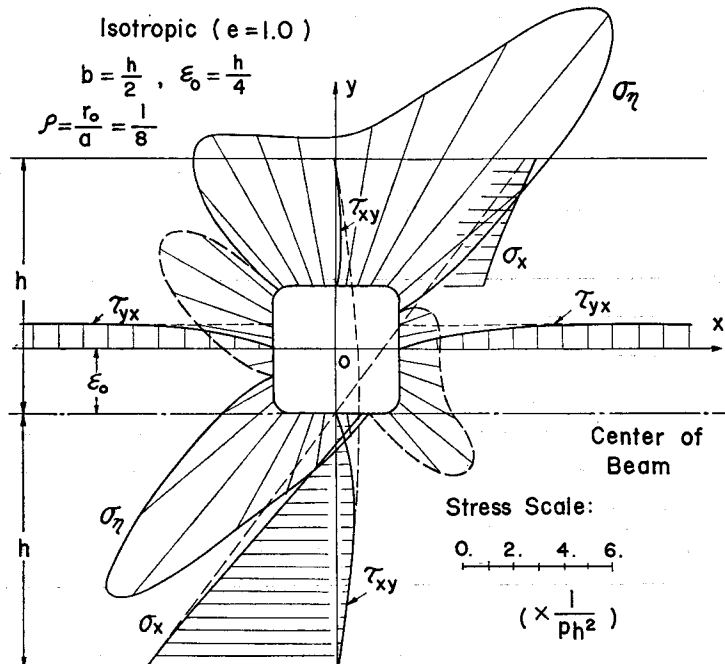
Fig. 11. Typical tangential stress distribution along edge of circular and elliptical ($a/b=2.0$) hole in an orthotropic cantilever beam subjected to a uniformly distributed load.

(4) Stresses at the Region of Exterior to the Hole Surface

In the previous examples we calculated only the distribution of circumferential stress σ_η at the contour of a hole which is perforated in an isotropic or an orthotropic beam under several external loads. Let us calculate here the stress distribution at the region exterior to the hole surface. Though the calculations in this case are very complicated compared with the previous treatments, the problems can be solved in the same manner as the above.

Fig. 12 is some examples of circumferential stress σ_η at the edge of a hole and stresses σ_x, τ_{xy} along the x - and y -axes under the loading condition (2). Fig. 12 (a) is the stress distribution of σ_η at the contour and along the coordinate axes when a square hole ($\rho=r_0/a=1/8, b=h/2$) is perforated with eccentricity ($\varepsilon_0=h/4$) in an isotropic beam. The dotted lines in this figure show the distribution of stresses $\sigma_{xy}^0, \tau_{xy}^0$ caused in the beam having no hole. In the case of an orthotropic beam having a circular hole ($b=h/2$) with eccentricity ($\varepsilon_0=h/4$), the stress distribution is shown in Fig. 12 (b).

Assuming that the problem under consideration can be treated as a single-connected region with a hole as mentioned in the first section, the boundaries of the upper and lower sides of a beam are neglected in above examples. In this place we consider the effect of these boundaries on the stress distribution in a beam having



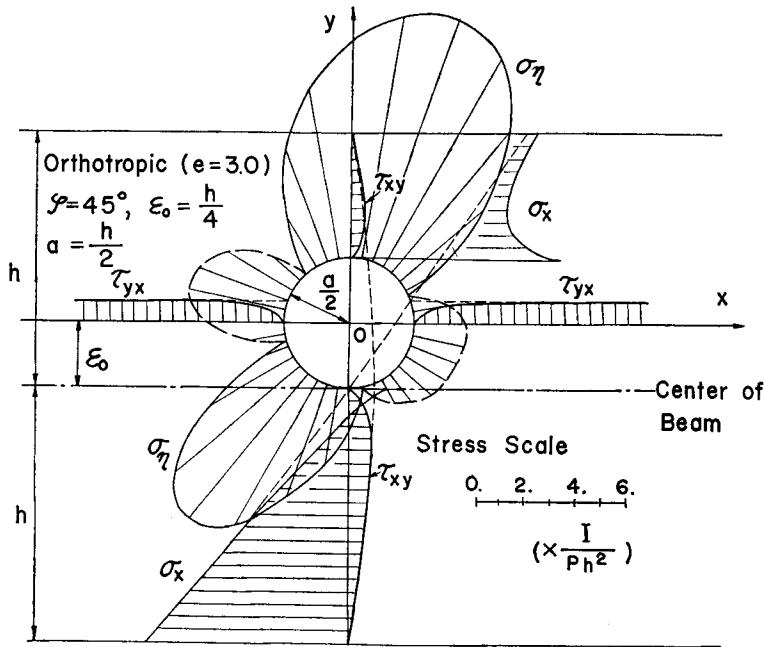


Fig. 12. Typical examples of stresses at the region of exterior of hole surface in cantilever beams subjected to a terminally concentrated load. (a) square hole ($\rho=r_0/a=1/8$, $b=h/2$, $\epsilon_0=h/4$) in an isotropic beam, (b) circular hole ($b=h/2$, $\epsilon_0=h/4$) in an orthotropic beam.

a hole. In the case of Fig. 12 there is close agreement between the stresses σ_x , τ_{xy} of the beam with a hole and the stresses σ_x^0 , τ_{xy}^0 of the beam with no hole at the boundary of the lower side, but there is a difference of 5.5% between both cases on the upper boundary of the beam. Fig. 13 shows the distribution of stresses σ_x , τ_{xy} on the co-

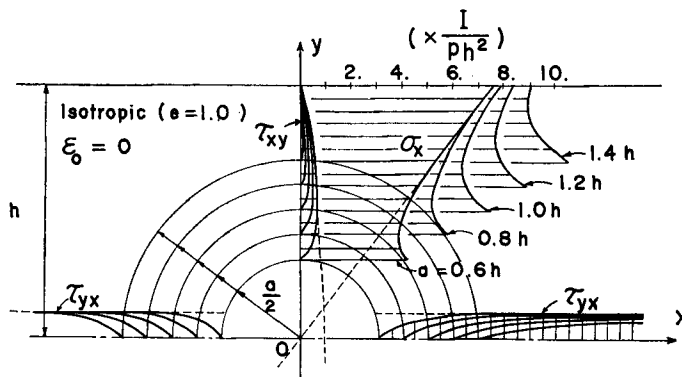


Fig. 13. Stresses σ_x , τ_{xy} on the coordinate axes of an isotropic cantilever beam with circular hole subjected to a terminally concentrated load.

ordinate axes under the loading condition of (2) in the case where the diameter of a circular hole located on the center line of an isotropic beam becomes large. From this figure, comparing stress σ_x with stress σ_y^0 along the y -axis on the upper boundary of the beam, we can observe the differences of 5.2% when the diameter of the hole becomes half of the width of beam (i.e. $b=h$) and 11% when $b=1.2h$.

Consequently, judging from the illustrations as in the problem of a single-connected region as treated in this paper and from many numerical examples not shown here, though some differences arise from individual cases (for example, condition of external loads, condition of the shape of a beam, ratio of elastic moduli of orthotropy, directions of principal elastic axes, size and shape of a hole, excentricity ϵ_0 or others), it may be thought that the results as above have an error within about 5% in the case that the hole is located within the range of $\pm h/2$ of the center line of the beam (width of the beam: $2h$).

(5) Stress Distribution Around Three Circular Holes Under Pure Bending

In the previous paper (reference 12), the author treated the theoretical solution by successive approximation to be obtained by the point matching approach using the solution of anisotropic elastic plate with an elliptical hole, and showed some numerical examples for an orthotropic plate containing two or three circular (or elliptical) holes. In some particular cases of isotropic or orthotropic plate with two or three equal circular holes, the results obtained by the method were quite in agreement with the results obtained by others. Thus by using the same method, we calculated the stress distribution at the contours of three circular holes located on the center line of an isotropic or an orthotropic beam under pure bending.

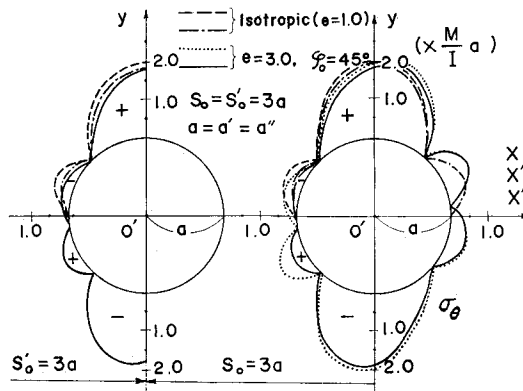


Fig. 14. Typical tangential stress distribution around three circular holes with equal radius in a line of the center line of an isotropic or an orthotropic beam subjected to pure bending.

Fig. 14 shows the stress distribution of σ_{η} , σ'_{η} around the right and the center holes in the case of an isotropic beam and in the case of an orthotropic beam containing three equal circular holes with the spacings $s_0/2a=s_1/2a=1.50$, subjected to end couples M .

5. Concluding Remarks

We investigated theoretically the effect of holes on the stress distribution in a homogeneous isotropic or anisotropic elastic beam subjected to bending with shear. In the process of this theoretical analysis, we used the stresses of an anisotropic beam based on the assumption of the Bernoulli-Euler's beam theory for an anisotropic elastic beam having no hole. Concerning this assumption, Hashin¹⁰⁾ has examined that the theoretical results are enough to be exact compared with the experimental ones of the maximum stress and the deflection of anisotropic beams.

We showed only the numerical examples of the stress distribution of isotropic or orthotropic beams having holes under three kinds of loading conditions, but it may be easily extended for any other loading conditions such as simple beams subjected to a concentrated load or to distributed loads.

Acknowledgement

I should like to express my indeptness to Dr. Y. Niwa for his suggestions on this problem and for much helpful advice.

References

- 1) Tuji, Z., Effect of a Circular Hole on the Stress Distribution Under Uniform Bending Moment, Sci. Paper of Inst. Phys. and Chem. Res., Tokyo, Vol. 9, (1928), pp. 65-89
- 2) Savin, G. N., Stress Concentration Around Holes, (translated from Russian by W. Johnson), Pergamon Press, (1961), pp. 87-104, 193-196
- 3) Joseph, J. A., and Brock, J. S., The Stresses Around a Small Opening in a Beam Subjected to Pure Bending, Jour. of Appl. Mech., Vol. 17, (1950), pp. 353-358
- 4) Heller, S. R., Jr., The Stresses Around a Small Opening in a Beam Subjected to Bending With Shear, Proc. 1st U. S. National Congr. Appl. Mech., Chicago, (1951), pp. 239-245
- 5) Heller, S. R., Jr., Brock, J. S., and Bart, R., The Stresses Around a Rectangular Opening With Rounded Corners in a Beam Subjected to Bending With Shear, Proc. 4th U. S. National Congr. Appl. Mech., Berkeley, (1962), pp. 489-496
- 6) Yamasaki, T., and Gotoh, K., Stresses Around a Hexagonal Hole With Rounded Corners in a Uniformly Loaded Rectangular Plate, Tech. Rep. of the Kyushu Univ., Vol. 41, (1968), pp. 931-938. (in Japanese)
- 7) Deresiewicz, H., Stresses in Beams Having Holes of Arbitrary Shape, Jour. of the Eng. Mech., ASCE, Vol. 94, No. EM-5, (1968), pp. 1183-1214

- 8) Lekhnitskii, S. G., *Anisotropic Plates*, (translated from Russian by S. W. Tsai and T. Cheron), Gordon and Breach Science Publishers, New York (1968), pp. 57–62, pp. 157–187
- 9) Silverman, I. K., *Orthotropic Beams Under Polynomial Loads*, *Jour. of the Eng. Mech., ASCE*, Vol. 90, No. EM-5, (1964), pp. 293–319
- 10) Hashin, Z., *Plane Anisotropic Beams*, *Jour. of Appl. Mech.*, Vol. 34 (1967) pp. 257–262
- 11) Green, A. E., and Zerna, W., *Theoretical Elasticity*, 2nd Ed., Oxford, (1968), pp. 362–368
- 12) Niwa, Y., and Hirashima, K., *Stress Distribution for Anisotropic Plate Containing Two or More Arbitrary Elliptical Holes*, *Mem. of the Fac. of Eng., Kyoto Univ.*, Vol. 33 (1971), pp. 101–117
- 13) Muskhelishvili, N. I., *Some Basic Problems of the Mathematical Theory of Elasticity*, (translated from Russian by J. R. M. Radok), Noordhoff, Holland, (1963), pp. 104–256
- 14) Neou, C. Y., *A Direct Method for Determining Airy Polynomial Stress Functions*, *Jour. of Appl. Mech.*, Vol. 24 (1957), pp. 387–390
- 15) Лехницкий, С.Г., *Анизотропные Пластинки*, Государственное Издательство Технико-Теоретической Литературы, Москва (1957) стр. 61–69.
- 16) Lekhnitskii, S. G., *Anisotropic Plates*, (translated from Russian by E. Z. Stowell), American Iron and Steel Institute, New York, (1956)
- 17) Heller, S. R., Jr., Brock, J. S., and Bart, R., *The Stresses Around a Rectangular Opening With Rounded Corners in a Uniformly Loaded Plate*, *Proc. 3rd U. S. National Congr. Appl. Mech.*, Providence (1958). pp. 357–368
- 18) Stephens, K. M., *A Boundary Problem in Orthotropic Generalized Plane Stress*, *Quart. Jour. Mech. and Appl. Math.*, Vol. 5 (1952), pp. 206–220
- 19) *ibid.* 8) pp. 235–272

Appendix I

In the case of an isotropic body, Muskhelishvili's complex variable method for solving two-dimensional elastic problems for a simple connected region consists of the determination of two analytic functions $\varphi(z_0)$ and $\psi(z_0)$ to represent the stress function. The first boundary-value problems for the functions $\varphi(z_0)$ and $\psi(z_0)$ have the following form:

$$z_0 \overline{\varphi'(z_0)} + \varphi(z_0) + \overline{\psi(z_0)} = - \int_0^s (iX_n - Y_n) ds + c. \quad (\text{A.1})$$

In which X_n , Y_n are the external stresses along the contour of the hole defined by equation (3.2); and c is an integration constant.

We denote the results of the substitution $z_0 = \omega(\zeta)$ in $\varphi(z_0)$ and $\psi(z_0)$ by $\varphi_1(\zeta_0)$ and $\psi_1(\zeta_0)$, respectively, so that

$$\varphi[\omega(\zeta)] \equiv \varphi_1(\zeta), \quad \psi[\omega(\zeta)] \equiv \psi_1(\zeta).$$

In this case the boundary condition (A.1) becomes:

$$\left. \begin{aligned} \frac{\omega(\sigma)}{\omega'(\sigma)} \overline{\varphi_1'(\sigma)} + \varphi_1(\sigma) + \overline{\psi_1(\sigma)} &= f_1^0 + if_2^0, \\ f_1^0 + if_2^0 &= - \int_0^s (iX_n - Y_n) ds, \end{aligned} \right\} \quad (\text{A.2})$$

where $\sigma = e^{i\beta}$ is the value of ζ on the boundary of the unit circle.

Since $\omega(\zeta)$ is a polynomial of degree ν , the function $\omega(\sigma)/\omega'(\sigma)$ can be represented as follows.

$$\frac{\omega(\sigma)}{\omega'(\sigma)} = \sum_{p=1}^{\nu} r_p^* \sigma^{-p} + \sum_{p=0}^{\infty} r_p \sigma^p, \quad (\text{A.3a})$$

where,

$$\left. \begin{aligned} r_p^* &= \frac{\alpha_p + i\beta_p}{\alpha_0}, \quad (p = \nu, \nu - 1) \\ r_p^* &= \frac{1}{\alpha_0} \left\{ (\alpha_p + i\beta_p) + \sum_{j=1}^{\nu-p-1} j r_{p+j+1}^* (\alpha_j - i\beta_j) \right\}, \\ &\quad (p = \nu - 2, \nu - 3, \dots, 1) \\ r_p &= \delta_1^p + \frac{1}{\alpha_0} \sum_{j=p+1}^{\nu+p-1} j r_{j-p+1}^* (\alpha_j - i\beta_j), \quad (p = 0, 1) \\ r_p &= \frac{1}{\alpha_0} \left\{ \sum_{j=p}^{\nu} j r_{j-p+1}^* (\alpha_j - i\beta_j) + \sum_{j=1}^{p-1} j r_{p-j-1} (\alpha_j - i\beta_j) \right\}, \\ &\quad (p = 2, 3, \dots, \nu - 1) \\ r_\nu &= \frac{1}{\alpha_0} \sum_{j=1}^{\nu} j r_{\nu-j-1} (\alpha_\nu - i\beta_\nu), \\ r_p &= \frac{1}{\alpha_0} \sum_{j=1}^{\nu} j r_{p-j-1} (\alpha_j - i\beta_j), \quad (p = \nu + 1, \nu + 2, \dots, \infty). \end{aligned} \right\} \quad (\text{A.3b})$$

In which the symbol δ_i^j , the Kronecker delta, is defined as having the value one if i equals j , zero if i differs from j .

Consequently, all parts of the Laurent expansion can be completely evaluated by the known constants α_0 , α_m and β_m .

The functions $\varphi_1(\zeta)$ and $\psi_1(\zeta)$ are analytic within the region under consideration, and can be assumed to be the forms of the power series.

$$\left. \begin{aligned} \varphi_1(\zeta) &= A \ln \zeta + \sum_{m=1}^{\infty} A_m \zeta^{-m}, \\ \psi_1(\zeta) &= B \ln \zeta + \sum_{m=0}^{\infty} B_m \zeta^{-m}. \end{aligned} \right\} \quad (\text{A.4})$$

From equations (A. 3a) and (A.4), we can calculate the left-hand side of equation (A.2) as follows.

$$\frac{\omega(\sigma)}{\omega'(\sigma)} \overline{\varphi_1'(\sigma)} + \varphi_1(\sigma) + \overline{\psi_1(\sigma)} = i(A - B) \theta + \sum_{p=0}^{\infty} C_p^* \sigma^{-p} + \sum_{p=1}^{\infty} C_p \sigma^{-p}, \quad (\text{A.5a})$$

where,

$$\left. \begin{aligned} C_p^* &= A_p, \quad (p = \nu - 1, \nu, \dots, \infty) \\ C_p^* &= A_p - \sum_{j=1}^{\nu-p-1} j \bar{A}_j \bar{r}_{j+p+1}^*, \quad (p = 1, 2, \dots, \nu - 2) \\ C_0^* &= \bar{B}_0 - \sum_{j=1}^{\nu-1} j \bar{A}_j \bar{r}_{j+1}^*, \\ C_1 &= \bar{B}_1 - \sum_{j=1}^{\nu} j \bar{A}_j \bar{r}_{j+1}^*, \\ C_p &= \bar{B}_p - \sum_{j=p}^{\nu+p-1} j \bar{A}_j \bar{r}_{j-p+1}^* - \sum_{j=1}^{p-1} j \bar{A}_j \bar{r}_{p-j-1}, \quad (p = 2, 3, \dots, \infty). \end{aligned} \right\} (\text{A.5b})$$

And we can obtain the right-hand side of equation (A. 2) by use of the right-hand side of equation (3.7) as follows.

$$f_1^0 + i f_2^0 = \frac{1}{2\pi} (Y - iX) \theta + \sum_{m=1}^{\infty} (\bar{a}_m + i\bar{b}_m) \sigma^{-m} + \sum_{m=1}^{\infty} (a_m + ib_m) \sigma^m, \quad (\text{A.6})$$

in which a_m, b_m and their conjugates are determined by the results of Appendix II. By inserting from (A.5) and (A.6) in equation (A.2), and on comparing the coefficients of like powers of σ^m , we obtain:

$$\left. \begin{aligned} A_p &= (\bar{a}_p + i\bar{b}_p), \quad (p = \nu - 1, \nu, \dots, \infty) \\ A_p &= \sum_{j=1}^{\nu-p-1} j \bar{A}_j \bar{r}_{j+p+1}^* + (\bar{a}_p + i\bar{b}_p), \quad (p = 1, 2, \dots, \nu - 2) \\ \bar{B}_p &= (a_p + ib_p) + \sum_{j=1}^{\nu+p-1} j \bar{A}_j \bar{r}_{j+1}^*, \quad (p = 0, 1) \\ \bar{B}_p &= (a_p + ib_p) + \sum_{j=p}^{\nu+p-1} j \bar{A}_j \bar{r}_{j-p+1}^* + \sum_{j=1}^{p-1} j \bar{A}_j \bar{r}_{p-j-1}, \\ &\quad (p = 2, 3, \dots, \infty) \end{aligned} \right\} (\text{A.7a})$$

After some simple algebra, the second equation of (A.7a) yields the following:

$$\begin{aligned} & \sum_{j=1}^p A_j \left\{ \delta_j^p - j \sum_{k=p+2}^{\nu} (k-p-1) r_k^* \bar{r}_{k-p+j}^* \right\} - \sum_{j=p+1}^{\nu+2} A_j \left\{ j \sum_{k=p+2}^{\nu+p-1} (k-p-1) r_k^* \bar{r}_{k+p+j}^* \right\} \\ &= (a_p + ib_p) + \sum_{j=1}^{\nu-p-1} j \bar{r}_{j+p+1}^* (a_j - ib_j), \quad (p = 1, 2, \dots, \nu-2). \end{aligned} \quad (\text{A.7b})$$

The solution of this system for the $A_1, A_2, \dots, A_{\nu-2}$ can be easily obtained.

On the other hand, the coefficients A and B are determined by comparison of the coefficient of θ in equations (A.5a) and (A.6) and by the condition of single-valuedness of displacements, so that

$$A = -\frac{X+iY}{2\pi(1+k)}, \quad B = +\frac{k(X-iY)}{2\pi(1+k)}. \quad (\text{A.8})$$

In which k is a constant defined as $k=(3-\nu_o)/(1+\nu_o)$ for plane stress. Therefore, all coefficients A , B , A_m and B_m of the functions $\varphi_1(\zeta)$ and $\psi_1(\zeta)$ are determined in terms of the known constants α_k , β_k , a_m and b_m .

Instead of determining the coefficients B_m by above equation, it is easier to proceed directly from the conjugate equation of (A.2), which gives

$$\psi_1(\zeta) = f_1 - if_2 + \bar{\varphi}_1(1/\zeta) - \frac{\omega(1/\zeta)}{\omega'(\zeta)} \varphi_1'(\zeta), \quad (\text{A.9a})$$

where,

$$f_1 - if_2 = \frac{1}{2\pi} (X-iY) \ln \zeta + \sum_{m=1}^{\infty} (a_m - ib_m) \zeta^m + \sum_{m=0}^{\infty} (\bar{a}_m - i\bar{b}_m) \zeta^{-m}. \quad (\text{A.9b})$$

Thus the stress components σ_x , σ_y and τ_{xy} in isotropic plate can be calculated by use of equations (2.6), (A.7) and (A.9) in the usual manner.

Appendix II

In order to obtain the coefficients \bar{a}_m and \bar{b}_m of complex functions $\phi_k(z_k)$ or $\varphi(z_o)$, $\psi(z_o)$, several integrations must be carried out. In this appendix, let us show some of the formulae of auxiliary integrations which are necessary to clarify the theoretical analysis.

We rewrite the expression (3.1) which represents the contour of an opening under consideration, as follows:

$$\left. \begin{aligned} x_o &= \sum_{m=1}^{\nu} (\alpha_m' \cos m\theta + \beta_m \sin m\theta), \\ y_o &= \sum_{m=1}^{\nu} (\alpha_m'' \sin m\theta + \beta_m \cos m\theta), \end{aligned} \right\} \quad (\text{A.10})$$

in which,

$$\left. \begin{aligned} \alpha_1' &= \alpha_0 + \alpha_1, \quad \alpha_1'' = \alpha_0 - \alpha_1, \\ \alpha_j' &= \alpha_j, \quad \alpha_j'' = -\alpha_j, \quad (j = 2, 3, \dots, \nu). \end{aligned} \right\} \quad (\text{A.11})$$

Then by differentiation of equation (A.9) with respect to variable θ , we obtain

$$\left. \begin{aligned} dx_o &= \sum_{m=1}^{\nu} m(-\alpha_m' \sin m\theta + \beta_m \cos m\theta) d\theta, \\ dy_o &= \sum_{m=1}^{\nu} m(\alpha_m'' \cos m\theta - \beta_m \sin m\theta) d\theta. \end{aligned} \right\} \quad (\text{A.12})$$

Using these expressions, the following integrations are not so difficult to obtain.

$$\left. \begin{aligned} \int y_o dy_o &= \frac{1}{2} \left\{ F_o^1 \theta + \sum_{m=1}^{2\nu} (F_m^1 \cos m\theta + H_m^1 \sin m\theta) \right\}, \\ \int y_o dx_o &= \frac{1}{2} \left\{ F_o^2 \theta + \sum_{m=1}^{2\nu} (F_m^2 \cos m\theta + H_m^2 \sin m\theta) \right\}, \\ \int x_o dx_o &= \frac{1}{2} \left\{ F_o^3 \theta + \sum_{m=1}^{2\nu} (F_m^3 \cos m\theta + H_m^3 \sin m\theta) \right\}, \end{aligned} \right\} \quad (\text{A.13})$$

where,

$$\left. \begin{aligned} F_o^1 &= 0, \quad F_o^2 = -F_o^3 = \sum_{j=1}^{\nu} j(\beta_j^2 - \alpha_j' \alpha_j''), \\ F_1^\alpha &= \sum_{j=2}^{\nu} (A_{j,j-1}^{\alpha,2} + A_{j-1,j}^{\alpha,2}), \quad H_1^\alpha = \sum_{j=2}^{\nu} (A_{j,j-1}^{\alpha,4} - A_{j-1,j}^{\alpha,4}), \\ F_n^\alpha &= \sum_{j=1}^{n-1} A_{n-j,j}^{\alpha,1} + \sum_{j=n+1}^{\nu} (A_{j,j-n}^{\alpha,2} + A_{j-n,j}^{\alpha,2}), \\ H_n^\alpha &= \sum_{j=1}^{n-1} A_{n-j,j}^{\alpha,3} + \sum_{j=n+1}^{\nu} (A_{j,j-n}^{\alpha,4} - A_{j-n,j}^{\alpha,4}), \\ &\quad (\text{for } n = 2, 3, \dots, \nu - 1) \\ F_n^\alpha &= \sum_{j=1}^{n-1} A_{n-j,j}^{\alpha,1}, \quad H_n^\alpha = \sum_{j=1}^{n-1} A_{n-j,j}^{\alpha,3}, \quad (\text{for } n = \nu, \nu + 1) \\ F_n^\alpha &= \sum_{j=n-\nu}^{\nu} A_{n-j,j}^{\alpha,1}, \quad H_n^\alpha = \sum_{j=n-\nu}^{\nu} A_{n-j,j}^{\alpha,3}, \quad (\text{for } n = \nu + 2, \dots, 2\nu) \\ &\quad \alpha = 1, 2, 3. \end{aligned} \right\} \quad (\text{A.14})$$

$$\left. \begin{aligned} A_{k,j}^{\alpha,1} &= \frac{j}{k+j} B_{k,j}^{\alpha,1}, \quad A_{k,j}^{\alpha,3} = -\frac{j}{k-j} B_{k,j}^{\alpha,2}, \\ A_{k,j}^{\alpha,3} &= \frac{j}{k+j} B_{k,j}^{\alpha,3}, \quad A_{k,j}^{\alpha,4} = -\frac{j}{k-j} B_{k,j}^{\alpha,4}. \end{aligned} \right\} \quad (\text{A.15})$$

$$\left. \begin{aligned} B_{k,j}^{1,1} &= \beta_k \beta_j - \alpha_k'' \alpha_j'', \quad B_{k,j}^{1,2} = \alpha_k'' \alpha_j'' + \beta_k \beta_j, \\ B_{k,j}^{1,3} &= \alpha_j'' \beta_k + \alpha_k'' \beta_j, \quad B_{k,j}^{1,4} = \alpha_k'' \beta_j - \alpha_j'' \beta_k. \end{aligned} \right\} \quad (\text{A.16a})$$

$$\left. \begin{aligned} B_{k,j}^{2,1} &= \alpha_j' \beta_k - \beta_j \alpha_k'', \quad B_{k,j}^{2,2} = \alpha_j' \beta_k + \beta_j \alpha_k'', \\ B_{k,j}^{2,3} &= \beta_j \beta_k + \alpha_j' \alpha_k'', \quad B_{k,j}^{2,4} = \alpha_j' \alpha_k'' - \beta_j \beta_k. \end{aligned} \right\} \quad (\text{A.16b})$$

$$B_{k,j}^{3,i} = B_{j,k}^{2,i}, \quad (i = 1, 2, 3, 4). \quad (\text{A.16c})$$

$$\left. \begin{aligned} \int y_o^2 dy_o &= \frac{1}{4} \left\{ M_o^1 \theta + \sum_{m=1}^{3\nu} (M_m^1 \cos m\theta + N_m^1 \sin m\theta) \right\}, \\ \int y_o^2 dx_o &= \frac{1}{4} \left\{ M_o^2 \theta + \sum_{m=1}^{3\nu} (M_m^2 \cos m\theta + N_m^2 \sin m\theta) \right\}, \\ \int x_o y_o dy_o &= \frac{1}{4} \left\{ M_o^3 \theta + \sum_{m=1}^{3\nu} (M_m^3 \cos m\theta + N_m^3 \sin m\theta) \right\}, \end{aligned} \right\} \quad (\text{A.17})$$

where,

$$\left. \begin{aligned} M_o^1 &= \sum_{j=1}^{\nu} j (V_j^1 \alpha_j'' - W_j^1 \beta_j), & M_o^2 &= \sum_{j=1}^{\nu} j (V_j^1 \beta_j - W_j^1 d_j), \\ M_o^3 &= \sum_{j=1}^{\nu} j (V_j^2 \alpha_j'' - W_j^2 \beta_j), \\ M_n^\alpha &= \sum_{j=1}^n J_{n-j,j}^{\alpha,3} + \sum_{j=1}^{\nu} J_{n+j,j}^{\alpha,4} + \sum_{j=n}^{\nu} J_{j-n,j}^{\alpha,4}, & (\text{for } n=1, 2, \dots, \nu) \\ N_n^\alpha &= \sum_{j=1}^n J_{n-j,j}^{\alpha,1} + \sum_{j=1}^{\nu} J_{n+j,j}^{\alpha,2} - \sum_{j=n}^{\nu} J_{j-n,j}^{\alpha,2}, \\ M_n^\alpha &= \sum_{j=1}^{\nu} J_{n-j,j}^{\alpha,3} + \sum_{j=n+1}^{2\nu} J_{j,j-n}^{\alpha,4}, & (\text{for } n=\nu+1, \nu+2, \dots, 2\nu-1) \\ N_n^\alpha &= \sum_{j=1}^{\nu} J_{n-j,j}^{\alpha,1} + \sum_{j=n+1}^{2\nu} J_{j,j-n}^{\alpha,2}, \\ M_{2\nu}^\alpha &= \sum_{j=1}^{\nu} J_{2\nu-j,j}^{\alpha,3}, & N_{2\nu}^\alpha &= \sum_{j=1}^{\nu} J_{2\nu-j,j}^{\alpha,1}, \\ M_n^\alpha &= \sum_{j=n-2\nu}^{\nu} J_{n-j,j}^{\alpha,3}, & N_n^\alpha &= \sum_{i=n-2\nu}^{\nu} J_{n-j,j}^{\alpha,1}, & (\text{for } n=2\nu+1, \dots, 3\nu) \\ & & \alpha &= 1, 2, 3. \end{aligned} \right\} \quad (\text{A.18})$$

$$\left. \begin{aligned} J_{k,j}^{1,1} &= \frac{j}{k+j} (V_k^1 \alpha_j'' + W_k^1 \beta_j), & J_{k,j}^{1,2} &= -\frac{j}{k-j} (V_k^1 \alpha_j'' - W_k^1 \beta_j), \\ J_{k,j}^{1,3} &= \frac{j}{k+j} (W_k^1 \alpha_j'' - V_k^1 \beta_j), & J_{k,j}^{1,4} &= -\frac{j}{k-j} (W_k^1 \alpha_j'' + V_k^1 \beta_j). \end{aligned} \right\} \quad (\text{A.19a})$$

$$\left. \begin{aligned} J_{k,j}^{2,1} &= \frac{j}{k+j} (V_k^1 \beta_j + W_k^1 \alpha_j'), & J_{k,j}^{2,2} &= -\frac{j}{k-j} (-V_k^1 \beta_j + W_k^1 \alpha_j'), \\ J_{k,j}^{2,3} &= \frac{j}{k+j} (V_k^1 \alpha_j - W_k^1 \beta_j), & J_{k,j}^{2,4} &= -\frac{j}{k-j} (W_k^1 \beta_j + V_k^1 \alpha_j'). \end{aligned} \right\} \quad (\text{A.19b})$$

$$\left. \begin{aligned} J_{k,j}^{3,1} &= \frac{j}{k+j} (V_k^2 \alpha_j'' + W_k^2 \beta_j), & J_{k,j}^{3,2} &= -\frac{j}{k-j} (W_k^2 \beta_j - V_k^2 \alpha_j''), \\ J_{k,j}^{3,3} &= \frac{j}{k+j} (V_k^2 \beta_j - W_k^2 \alpha_j''), & J_{k,j}^{3,4} &= -\frac{j}{k-j} (W_k^2 \alpha_j'' + V_k^2 \beta_j). \end{aligned} \right\} \quad (\text{A.19c})$$

$$\begin{aligned}
V_0^\alpha &= \sum_{j=1}^{\nu} B_{j,j}^{\alpha,2}, \\
V_1^\alpha &= \sum_{j=2}^{\nu} (B_{j,j-1}^{\alpha,2} + B_{j-1,j}^{\alpha,2}), \quad W_1^\alpha = \sum_{j=2}^{\nu} (B_{j,j-1}^{\alpha,4} - B_{j-1,j}^{\alpha,4}), \\
V_n^\alpha &= \sum_{j=1}^{n-1} B_{n-j,j}^{\alpha,1} + \sum_{j=n+1}^{\nu} (B_{j,j-n}^{\alpha,2} + B_{j-n,j}^{\alpha,2}), \\
&\hspace{25em} (\text{for } n = 2, 3, \dots, \nu-1) \\
W_n^\alpha &= \sum_{j=1}^{n-1} B_{n-j,j}^{\alpha,3} + \sum_{j=n+1}^{\nu} (B_{j,j-n}^{\alpha,4} - B_{j-n,j}^{\alpha,4}), \\
V_n^\alpha &= \sum_{j=1}^{n-1} B_{n-j,j}^{\alpha,1}, \quad W_n^\alpha = \sum_{j=1}^{n-1} B_{n-j,j}^{\alpha,3}, \quad (\text{for } n = \nu, \nu+1) \\
V_n^\alpha &= \sum_{j=n-\nu}^{\nu} B_{n-j,j}^{\alpha,1}, \quad W_n^\alpha = \sum_{j=n-\nu}^{\nu} B_{n-j,j}^{\alpha,3}, \quad (\text{for } n = \nu+2, \dots, 2\nu) \\
&\hspace{15em} \alpha = 1, 2.
\end{aligned} \tag{A.20}$$